

Wall effect on pressure drop in packed beds

Cheng, Nian-Sheng

2011

Cheng, N. S. (2011). Wall effect on pressure drop in packed beds. *Powder Technology*, 210(3), 261-266.

<https://hdl.handle.net/10356/83906>

<https://doi.org/10.1016/j.powtec.2011.03.026>

© 2011 Elsevier. This is the author created version of a work that has been peer reviewed and accepted for publication by Powder Technology, Elsevier. It incorporates referee's comments but changes resulting from the publishing process, such as copyediting, structural formatting, may not be reflected in this document. The published version is available at: [DOI: <http://dx.doi.org/10.1016/j.powtec.2011.03.026>].

Downloaded on 04 Feb 2023 03:56:22 SGT

Wall effect on pressure drop in packed beds

*Nian-Sheng Cheng **

*School of Civil Environmental Engineering, Nanyang Technological University, Singapore 639798,
Singapore*

* Fax: +65 67910676. E-mail address: cnscheng@mtu.edu.sg

ABSTRACT

The wall effect on the pressure drop in packed beds could be considered by modifying the Ergun equation based on the concept of hydraulic radius. However, the prediction of the two constants involved in the modified Ergun equation, if using the correlations available in the literature, could differ significantly from one another, and all correlations are not applicable for very low bed-to-particle diameter ratios. In this study, a capillary-type model is proposed to be composed of a bundle of capillary tubes subject to a series of local energy losses, the latter being simulated in terms of sphere drag. The formulas derived provide a good description of variations in the two constants for bed-to-particle diameter ratios ranging from 1.1 to 50.5.

Keywords: Packed bed, Pressure drop, Ergun equation, Wall effect, Hydraulic radius

1. Introduction

The pressure drop for flow through a packed bed of spheres can be evaluated using the Ergun equation [1], i.e.

$$\frac{\Delta P}{L} = A_E \frac{(1-\varepsilon)^2 \rho \nu U}{\varepsilon^3 d^2} + B_E \frac{1-\varepsilon \rho U^2}{\varepsilon^3 d} \quad (1)$$

where ΔP is the pressure drop, L is the bed length, U is the superficial flow velocity (i.e. volumetric flow rate divided by the cross-sectional area of the bed), ρ is the fluid density, ν is the kinematic viscosity of fluid, d is the particle diameter, ε is the average porosity, $A_E = 150$ and $B_E = 1.75$. In terms of the pore-based friction factor and Reynolds number, Eq. (1) can be rewritten to be [2]

$$f_E = \frac{A_E}{Re_E} + B_E \quad (2)$$

where f_E is the friction factor,

$$f_E = \frac{\varepsilon^3 d \Delta P}{(1-\varepsilon)\rho U^2 L} = \frac{\varepsilon d}{(1-\varepsilon)} \frac{\Delta P}{\rho (U/\varepsilon)^2 L} \quad (3)$$

and Re_E is the Reynolds number,

$$Re_E = \frac{Ud}{\nu(1-\varepsilon)} = \frac{\varepsilon d}{(1-\varepsilon)} \frac{U/\varepsilon}{\nu}. \quad (4)$$

By noting that the hydraulic radius for packed spheres is $R = \varepsilon d / [6(1-\varepsilon)]$, which measures the average length scale of the pore, and the average velocity of flow through pores is $U_p (=U/\varepsilon)$, f_E and Re_E serve as the distinctive parameters for describing flows through the fictitious pipe that is characterised with the section dimension $\varepsilon d / (1-\varepsilon)$ and average velocity U_p .

The Ergun equation applies only for the packed bed with negligible wall effects. If the bed diameter D is not large in comparison to the sphere diameter, say, $D/d < 40$, the pressure drop predicted by the Ergun equation would differ significantly from measurements [3]. Such wall effects on the pressure drop in packed beds have received limited attention, in spite of the fact that a great deal of studies has been conducted for flows through porous media.

The wall effect is twofold. In the creeping flow regime, the pressure drop may be increased due to the additional wall friction, of which the effect is dominant in comparison to the increased porosity. On the other hand, in turbulent flows, the pressure drop might be reduced due to the increase

in the near-wall porosity [4,5]. In other words, the wall effect is Reynolds number dependent. An increased pressure drop due to wall effect is usually associated with creeping flows, while the reduced pressure drop occurs at high Reynolds numbers. Experimental observations in this respect have been reviewed by Einfeld and Schnitzlein [4].

A simple wall correction approach was proposed early by Mehta and Hawley [6] by modifying the hydraulic radius as

$$R = \frac{1 - \varepsilon}{6} \frac{d}{M} \quad (5)$$

where M is the modification factor,

$$M = 1 + \frac{2}{3} \frac{1 - \varepsilon}{D} \frac{d}{D} \quad (6)$$

Using the modified hydraulic radius, Eq. (2) is revised to be

$$f_w = \frac{A_w}{Re_w} + B_w \quad (7)$$

or

$$f_E = \frac{A_w M^2}{Re_E} + B_w M \quad (8)$$

where $f_w = f_E/M$, $Re_w = Re_E/M$, and A_w and B_w are constants. Comparison of Eqs. (2) and (8) yields that $A_E = A_w M^2$ and $B_E = B_w M$.

Mehta and Hawley [6] showed that Eq. (7) with $A_w = 150$ and $B_w = 1.75$ fits well to experimental data for $D/d = 7.7-91$. However, Foumeny et al. [7] noted that Mehta and Hawley's approach overestimated the pressure drop by over 100% at $D/d=3.5$. Reichelt [8]

argued that A_w remained constant but B_w reduced with decreasing D/d , which for spheres is empirically expressed as

$$B_w = \left[\frac{1.5}{(D/d)^2} + 0.88 \right]^{-2}. \quad (9)$$

Eisfeld and Schnitzlein [4] showed that Eq. (9) with slightly adjusted constants performs better than several other pressure drop correlations for $D/d = 1.624$ – 250 . Fand and Thinakaran [9] reported that both A_w and B_w increase with increasing D/d in similar forms for $D/d = 1.40$ – 41.28 . However, such variations reverse for very small D/d . Fand et al. [10] observed that A_w and B_w decrease with increasing D/d for $D/d = 1.08$ – 1.40 . Similar experiments for very low ratios of D/d have also been conducted by Calis et al. [11] and Cheng et al. [12] for square packed beds. Montillet and Comiti [13] commented that both porosity and bed-to-particle diameter ratio should be used to take wall effects into account in relating friction factor to Reynolds number.

Table 1 summarises various correlations available in the literature for evaluating A_w and B_w . The formulas by Foumeny et al. [7], Raichura [14] and Montillet and Comiti [13] are obtained by reformulating their original correlations for very small or large Reynolds numbers in terms of f_w and Re_w . Plotted in Figs. 1 and 2 are the A_w - and B_w -correlations, respectively, in comparison with the experimental results presented by Fand and Thinakaran [9] and Fand et al. [10]. Fand and his colleagues provided two sets of A_w and B_w , which were evaluated for Forchheimer and turbulent flow, respectively. Both data are plotted in Figs. 1 and 2, showing fluctuations inherent in the two coefficients. Eisfeld and Schnitzlein's [4] correlation is very close to that by Reichelt [8] and thus ignored in the figures.

Fig. 1 shows that the data for $D/d > 1.4$ could be approximated as a constant, as suggested by Mehta and Hawley [6] and Reichelt [8], while the increasing trend of A_w with increasing D/d is predicted by Foumeny et al. [7] and Montillet and Comiti [13]. However, Raichura's [14] A_w -prediction is much greater than the others and also the data. From Fig. 2, it follows that similar to the data for $D/d > 1.4$, Reichelt [8], Foumeny et al. [7], Raichura [14] and Montillet and

Comiti [13] all predict the increasing trend of B_w with increasing D/d , in spite of the different deviations from the data.

Furthermore, it should be mentioned that both Figs. 1 and 2 clearly show that all correlations are not applicable for very small values of D/d , say, $D/d < 1.4$. As d gradually approaches D , both A_w and B_w increase significantly, in comparison to the opposite variation observed for $D/d > 1.4$.

Though the wall effect could be taken into account by modifying the hydraulic radius, no acceptable theory or experimental correlation has been established for evaluating A_w and B_w . On the other hand, to understand fluid mechanics implied by the Ergun equation, various theoretical efforts, such as integrated one-dimensional model (which is concerned here) and differential three-dimensional analysis, have been developed in the literature.

For example, Niven [15] employed a simplified model of pore conduit, which is subject to a series of expansions and contractions, and expressed the energy loss as a sum of frictional (laminar or turbulent) losses along the straight conduit and local losses due to the expansions and contractions. Blick [16] modelled the constrictions as a series of orifice plates and thus evaluated the packed bed friction as pipe friction modified by the orifice-induced drag. This so-called capillary–orifice model comprised of two parts, a bundle of capillary tubes and a series of orifice plates spaced along the distance interval equivalent to the mean pore diameter. By applying this model, the problem of predicting pressure drops in porous media reduces to one of determining skin friction coefficients related to the capillary tubes and drag coefficients associated with the orifice plates. Blick's work was further developed recently by Choi et al. [17], who evaluated the orifice diameter and thus drag coefficient by considering two types of simplified pore structures. Choi et al. demonstrated that the effect of increased porosity near the wall, which is significant at high Reynolds numbers, could be taken into account by introducing a drag-based correction coefficient in the inertial term of the Ergun equation. Both Blick [16] and Choi et al. [17] show that the capillary–orifice model is very sensitive to the evaluation of the orifice diameter and its discharge coefficient, which is generally difficult depending on how to properly simplify the bed configuration.

This note aims to develop an approach for evaluating A_w and B_w for a wide range of D/d . By following the ideas presented by Blick [16] and Niven [15], we also assume that the pressure drop comprises two components, the first being simulated by the fictitious pipe friction and the other being represented by the local drag or loss. However, the drag induced by the orifice plates or the local loss by sudden expansions and contractions is replaced here with that by spheres.

2. Present consideration

Consider a bed of packed spheres, of which the length is L and the cross-sectional area is A . Through the bed, the pressure drop is ΔP , and its non-dimensional form is expressed as the energy slope or hydraulic gradient, S [$= \Delta P/(\rho g L)$]. Similar to ΔP , the energy slope is assumed to have two parts. The first part S_f is related to the fictitious pipe friction. Using the pore-based velocity or average interstitial velocity U_p and hydraulic radius R , S_f is expressed as

$$S_f = \frac{f U_p^2}{8gR} = \frac{3f U_p^2}{4} \frac{1-\varepsilon}{\varepsilon d} \quad (10)$$

where f is the friction factor for the fictitious pipe. The second part S_L represents the local loss, which is approximated to be proportional to sphere drag. In the control volume $A \times L$, the number of packed spheres is $N = AL(1-\varepsilon)/(\pi d^3/6)$. The total drag induced by spheres is NF_D , where F_D is the drag force of a sphere. By approximating F_D as $C_D(\pi d^2/4)(\rho U_p^2/2)$, where C_D is the equivalent drag coefficient associated with the local loss, S_L can be then expressed as the drag-related local energy loss per unit weight of fluid, i.e.

$$S_L = \frac{NF_D}{AL\varepsilon\rho g} = \frac{3C_D}{4} \frac{1-\varepsilon}{\varepsilon} \frac{U_p^2}{gd} \quad (11)$$

Therefore, the total energy slope is

$$S = S_f + S_L = \frac{3(f + C_D) 1 - \varepsilon U_p^2}{4 \varepsilon g d} \quad (12)$$

and the corresponding friction factor is

$$f_E = \frac{\varepsilon d S g}{(1 - \varepsilon) U_p^2} = \frac{3}{4} (f + C_D). \quad (13)$$

To evaluate f and C_D included in Eq. (13), the knowledge of pipe flow and sphere drag is applied. Although the friction function for regular pipe flows and the drag coefficient related to isolated sphere are generally not applicable for the packed bed model here, the fundamental relationships in terms of dimensionless parameters would remain for very small or large Reynolds numbers.

2.1. Friction factor for fictitious pipe

Consider two extreme cases. For the creeping flow at very low Reynolds numbers, the pipe friction factor can be expressed as

$$f_L = \frac{C_1}{Re} \quad (14)$$

where C_1 is a constant. By taking $Re = 4U_p R/\nu$ and $R = \varepsilon d/[6(1-\varepsilon)]$,

$$f_L = C_2 \frac{(1-\varepsilon)\nu}{\varepsilon U_p d} \quad (15)$$

where C_2 is a constant.

On the other hand, if the inertial effect is dominant at high Reynolds numbers, the friction factor is a function of the relative roughness height, which is in the order of R/d or $(1-\varepsilon)/\varepsilon$. A further approximation can be made based on the observation of flow resistance in

rough open channels. For the latter, the ratio of the mean velocity V to shear velocity u_* can be empirically related to the relative roughness height [18],

$$\frac{V}{u_*} = C_3 \left(\frac{R}{k_s} \right)^{1/6} \quad (16)$$

where C_3 is a constant, R is the hydraulic radius and k_s is the roughness height that is in the order of the grain size d . In terms of friction factor, Eq. (16) can be rewritten as

$$f_H = C_4 \left(\frac{1-\varepsilon}{\varepsilon} \right)^{1/3} \quad (17)$$

where C_4 is a constant, and subscript H denotes high Reynolds number.

2.2. Drag coefficient for spheres

In a packed bed, a sphere is confined by its identical neighbours and thus the modified drag differs from that for an isolated sphere. However, it is still reasonable to assume that the fundamental relations, except for the numerical coefficients, remain at least for two extreme regimes, i.e. creeping flow and inertia-dominant flow.

In the regime of creeping flow, the drag coefficient is assumed inversely proportional to the Reynolds number,

$$C_{DL} = E_1 \frac{\nu}{U_p d} \quad (18)$$

where E_1 is a constant. If the inertial effect at high Reynolds numbers is dominant, the drag coefficient is independent of the Reynolds number,

$$C_{DH} = E_2 \quad (19)$$

where E_2 is a constant.

Furthermore, it is noted that the drag is increased for a single particle settling in a confined tube. The previous studies on the confined settling [18] suggested that the ratio of the reduced settling velocity to that with no wall restriction is proportional to $(D-d) / D$. Therefore, it may be assumed that the increased drag coefficient C_{Dw} in the presence of wall is related to C_D as follows,

$$C_{Dw} = E_3 C_D \left(\frac{D}{D-d} \right)^m \quad (20)$$

where E_3 is a coefficient and m is an exponent.

2.3. Formulas for evaluating A_w and B_w

For the case of low Reynolds numbers, using Eqs. (15) and (18) with C_D replaced by C_{Dw} given in Eq. (20), Eq. (13) can be rewritten as

$$f_{EL} = \frac{3}{4}(f_L + C_{DL}) = \alpha_1 \frac{v}{U_p d} \frac{1-\varepsilon}{\varepsilon} + \alpha_2 \frac{v}{U_p d} \left(\frac{D}{D-d} \right)^m \quad (21)$$

where α_1 and α_2 are constants. Comparing Eq. (21) with Eq. (2) for low Reynolds number yields

$$A_E = \alpha_1 + \alpha_2 \frac{\varepsilon}{1-\varepsilon} \left(\frac{D}{D-d} \right)^m \quad (22)$$

and thus

$$A_w = \left[\alpha_1 + \alpha_2 \frac{\varepsilon}{1-\varepsilon} \left(\frac{D}{D-d} \right)^m \right] \frac{1}{M^2}. \quad (23)$$

Similarly, for the case of high Reynolds numbers, using Eqs. (17) and (19) with C_D replaced by C_{Dw} given in Eq. (20), Eq. (13) is rewritten as

$$f_{EH} = \frac{3}{4}(f_H + C_{DH}) = \beta_1 \left(\frac{1-\varepsilon}{\varepsilon} \right)^{1/3} + \beta_2 \left(\frac{D}{D-d} \right)^m \quad (24)$$

where β_1 and β_2 are constants. By comparing Eq. (24) with Eq. (2) for high Reynolds numbers, one gets

$$B_E = \beta_1 \left(\frac{1-\varepsilon}{\varepsilon} \right)^{1/3} + \beta_2 \left(\frac{D}{D-d} \right)^m \quad (25)$$

and thus

$$B_w = \left[\beta_1 \left(\frac{1-\varepsilon}{\varepsilon} \right)^{1/3} + \beta_2 \left(\frac{D}{D-d} \right)^m \right] \frac{1}{M}. \quad (26)$$

In the foregoing section, both A_w and B_w are formulated by considering pipe friction and sphere drag for the extreme conditions. However, it should be noted that no particular values of the relevant friction factor and drag coefficient are used in the analysis. Instead, the five unknown parameters, α_1 , α_2 , β_1 , β_2 and m , included in Eqs. (23) and (26) are to be calibrated using experimental data collected for confined packed beds. This is detailed in the following section.

3. Comparisons

From Eqs. (23) and (26), it follows that both A_w and B_w depend on both ε and D/d . In general, the average porosity increases with reducing D/d though different packing configuration may lead to porosity variation for given D/d . Fig. 3 plots various measurements of the porosity, together with the relevant formulas presented previously [7,10,17]. It is

interesting to note that the measurements reported by Calis et al. [11] and Cheng et al. [12] for square packed beds are also consistent with the data measured for circular packed beds.

With the data presented in Fig. 3, the following formula is proposed to empirically describe the relationship between ε and D/d ,

$$\varepsilon = \left(\varepsilon_1^{-3} + \varepsilon_2^{-3} \right)^{-1/3} \quad (27)$$

where ε_1 is an asymptote for small D/d ,

$$\varepsilon_1 = 0.8 \left(\frac{D-d}{d} \right)^{0.27} \quad (28)$$

and ε_2 approximates the D/d -dependence for large D/d ,

$$\varepsilon_2 = 0.38 \left[1 + \left(\frac{d}{D-d} \right)^{1.9} \right]. \quad (29)$$

It should be noted that the porosity in the near-wall region, say, $D/d < 2$ may strongly depend on channel shape and the location of the peak porosity may also vary.

With the porosity calculated using Eq. (27), Eqs. (23) and (26) are compared with the experimental data provided largely by Fand and Thinakaran [9] and Fand et al. [10], as shown in Figs. 4 and 5, respectively. Additional data points plotted in the figures are due to Reichelt [8], Calis et al. [11] and Cheng et al. [12]. Both Calis et al. [11] and Cheng et al. [12] investigated spheres packed in square tubes. Calis et al. [11] performed experiments for flows at medium Reynolds numbers, and then extrapolated experimental results with CFD techniques to the flows at low and high Reynolds numbers. In comparison, Cheng et al.'s [12] experiments were conducted for a wide range of Reynolds number ($=Ud/\nu$), which varied from 2 to 5550 covering both linear and nonlinear flow regimes. From their results, the two constants, A_w and B_w , are calculated, as summarised in Table 2. Here, the pipe diameters are calculated by

considering equivalent circular pipes with the same cross-sectional areas of the square tubes, and the correction factor M is taken to be $1 + 2 d/[3(1-\varepsilon)s]$, where s is the side of the square cross section.

By trial and error, we get $\alpha_1 = 185$, $\alpha_2 = 17$, $\beta_1 = 1.3$, $\beta_2 = 0.03$ and $m = 2$. As shown in Figs. 4 and 5, Eqs. (23) and (26) represent well the experimental data in the wide range of D/d . However, further improvement could be made if more data are available, in particular, for small values of D/d .

4. Conclusions

In applying the Ergun equation to the evaluation of pressure drop in packed beds of limited size, the two constants involved can be modified based on the concept of hydraulic radius. However, the two constants cannot be predicted correctly using the correlations available in the literature, in particular for very low bed-to-particle diameter ratios. In this study, a capillary-type model is assumed to comprise a bundle of capillary tubes subject to a series of local energy losses, which is represented by sphere drag. Using the model, the dependence of the two constants on porosity and bed-to-particle diameter ratio is formulated. Being compared with experimental data of packed spheres, the formulas proposed describe the wall affected constants well for bed-to-particle diameter ratios ranging from 1.1 to 50.5.

References

- [1] S. Ergun, Fluid flow through packed columns, *Chemical Engineering Progress* 48 (1952) 9–94.
- [2] R.B. Bird, W.E. Stewart, E.N. Lightfoot, *Transport Phenomena*, 2nd ed. J. Wiley, New York, 2002.
- [3] M. Winterberg, E. Tsotsas, Impact of tube-to-particle-diameter ratio on pressure drop in packed beds, *AIChE Journal* 46 (5) (2000 May) 1084–1088.
- [4] B. Eisfeld, K. Schnitzlein, The influence of confining walls on the pressure drop in packed beds, *Chemical Engineering Science* 56 (14) (2001 Jul) 4321–4329.
- [5] R. Di Felice, L.G. Gibilaro, Wall effects for the pressure drop in fixed beds, *Chemical Engineering Science* 59 (14) (2004 Jul) 3037–3040.
- [6] D. Mehta, M.C. Hawley, Wall effect in packed columns, *Industrial & Engineering Chemistry Process Design and Development* 8 (2) (1969) 280–282.
- [7] E.A. Foumeny, F. Benyahia, J.A.A. Castro, H.A. Moallemi, S. Roshani, Correlations of pressure-drop in packed-beds taking into account the effect of confining wall, *International Journal of Heat and Mass Transfer* 36 (2) (1993 Jan) 536–540.
- [8] W. Reichelt, Calculation of pressure-drop in spherical and cylindrical packings for single-phase flow, *Chemie Ingenieur Technik* 44 (18) (1972) 1068–1071.
- [9] R.M. Fand, R. Thinakaran, The influence of the wall on flow through pipes packed with spheres, *Journal of Fluids Engineering-Transactions of the ASME* 112 (1) (1990 Mar) 84–88.
- [10] R.M. Fand, M. Sundaram, M. Varahasamy, Incompressible fluid-flow through pipes packed with spheres at low dimension ratios, *Journal of Fluids Engineering-Transactions of the ASME* 115 (1) (1993 Mar) 169–172.
- [11] H.P.A. Calis, J. Nijenhuis, B.C. Paikert, F.M. Dautzenberg, C.M. van den Bleek, CFD modelling

- and experimental validation of pressure drop and flow profile in a novel structured catalytic reactor packing, *Chemical Engineering Science* 56 (4) (2001 Feb) 1713–1720.
- [12] N.S. Cheng, Z.Y. Hao, S.K. Tan, Comparison of quadratic and power law for nonlinear flow through porous media, *Experimental Thermal and Fluid Science* 32 (8) (2008 Sep) 1538–1547.
- [13] A. Montillet, E. Akkari, J. Comiti, About a correlating equation for predicting pressure drops through packed beds of spheres in a large range of Reynolds numbers, *Chemical Engineering and Processing* 46 (4) (2007 Apr) 329–333.
- [14] R.C. Raichura, Pressure drop and heat transfer in packed beds with small tube-to-particle diameter ratio, *Experimental Heat Transfer* 12 (4) (1999 Oct–Dec) 309–327.
- [15] R.K. Niven, Physical insight into the Ergun and Wen & Yu equations for fluid flow in packed and fluidised beds, *Chemical Engineering Science* 57 (3) (2002 Feb) 527–534.
- [16] E.F. Blick, Capillary–orifice model for high-speed flow through porous media, *Industrial & Engineering Chemistry Process Design and Development* 5 (1) (1966) 90–94.
- [17] Y.S. Choi, S.J. Kim, D. Kim, A semi-empirical correlation for pressure drop in packed beds of spherical particles, *Transport in Porous Media* 75 (2) (2008 Nov) 133–149.
- [18] N. Qian, Z. Wan, *Mechanics of Sediment Transport*, American Society of Civil Engineers, Reston, Va, 1999.

List of Tables

Table 1 Empirical formulas proposed for evaluating A_w and B_w .

Table 2 A_w and B_w for spheres packed in square tube.

List of Figures

- Fig. 1 Variation of A_w with D/d . The circles denote the data for Forchheimer flow, and the triangles denote those for turbulent flow.
- Fig. 2 Variations of B_w with D/d . The circles denote the data for Forchheimer flow, and the triangles denote those for turbulent flow.
- Fig. 3 Variation of porosity with D/d , in comparison with Eq. (27).
- Fig. 4 Comparison of Eq. (23) (with $\alpha_1 = 185$, $\alpha_2 = 17$ and $m = 2$) with data. The circles denote the data for Forchheimer flow, and the triangles denote those for turbulent flow.
- Fig. 5 Comparison of Eq. (26) (with $\beta_1 = 1.3$, $\beta_2 = 0.03$ and $m = 2$) with data. The circles denote the data for Forchheimer flow, and the triangles denote those for turbulent flow.

Investigator	A_w	B_w	D/d
Mehta and Hawley [6]	150	1.75	7-91
Reichelt [8]	150	$\left[\frac{1.5}{(D/d)^2} + 0.88\right]^{-2}$	1.73-91
Foumeny et al. [7]	$\frac{130}{M^2}$	$\frac{D/d}{2.28 + 0.335(D/d)} \frac{1}{M}$	3.23-23.80
Raichura [14]	$\frac{103}{M^2} \left(\frac{\varepsilon}{1-\varepsilon}\right)^2 \left[6(1-\varepsilon) + \frac{80}{D/d}\right]$	$\frac{2.8}{M} \frac{\varepsilon}{1-\varepsilon} \left(1 - \frac{1.82}{D/d}\right)^2$	5-50
Eisfeld and Schnitzlein [4]	154	$\left[\frac{1.15}{(D/d)^2} + 0.87\right]^{-2}$	1.624-250
Montillet and Comiti [13]	$\frac{1000a}{M^2} \left(\frac{D}{d}\right)^{0.2} \frac{1}{1-\varepsilon}$	$\frac{12a}{M} \left(\frac{D}{d}\right)^{0.2}$	3.8-14.5
	where a = 0.061 for dense packing and 0.050 for loose packing.		
This study	$\left[185 + 17 \frac{\varepsilon}{1-\varepsilon} \left(\frac{D}{D-d}\right)^2\right] \frac{1}{M^2}$	$\left[1.3 \left(\frac{1-\varepsilon}{\varepsilon}\right)^{1/3} + 0.03 \left(\frac{D}{D-d}\right)^2\right] \frac{1}{M}$	

Table 1

Investigator	Ratio of square side to d	Equivalent D/d	ε	A_w	B_w	A_E	B_E
Calis et al. [11]	1.00	1.13	0.48	166.5	0.377	867.1	0.861
	1.15	1.30	0.60	128.3	0.269	769.4	0.659
	1.47	1.66	0.68	81.9	0.275	478.5	0.665
	2	2.26	0.48	126.0	0.488	339.3	0.801
	2	2.26	0.54	240.8	0.780	716.1	1.345
Cheng et al. [12]	1.025	1.16	0.50	127.3	0.410	674.0	0.95

Table 2

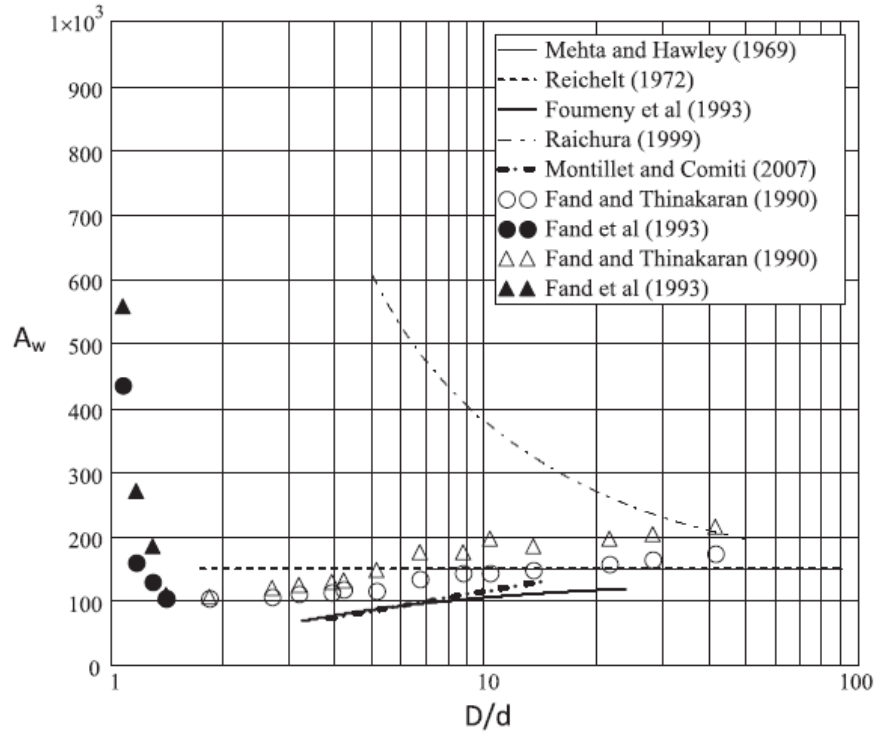


Fig. 1

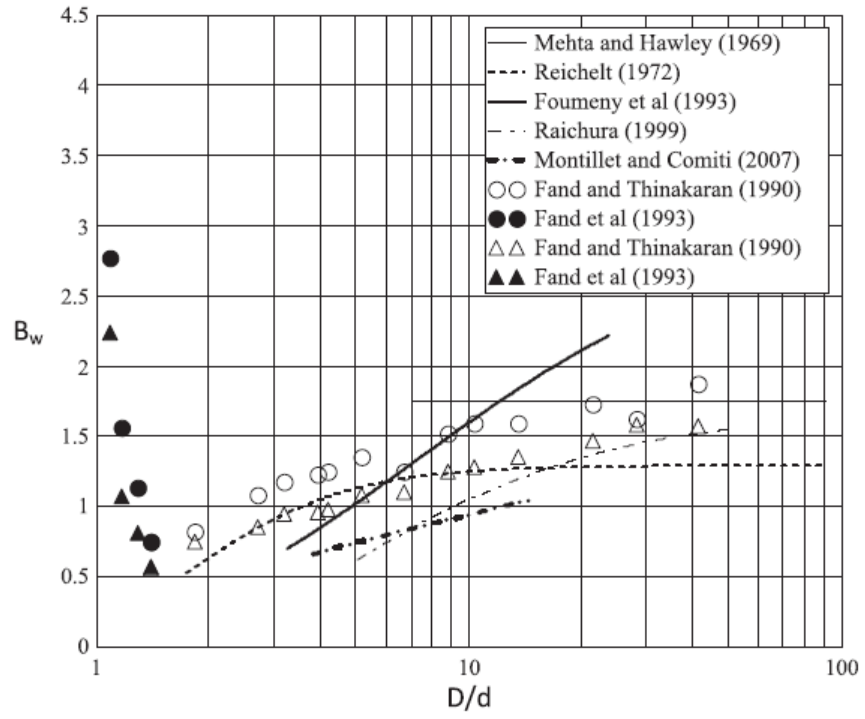


Fig. 2

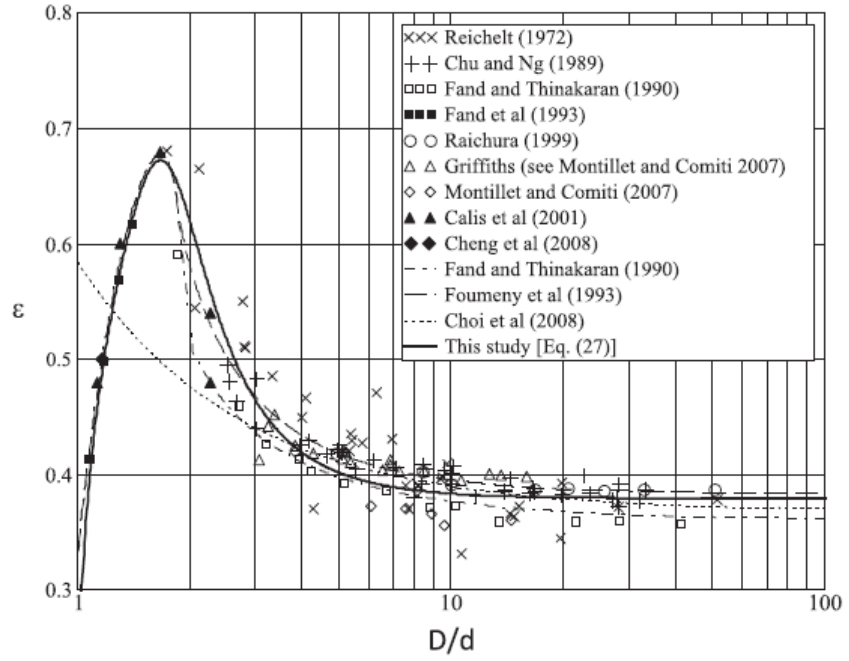


Fig. 3

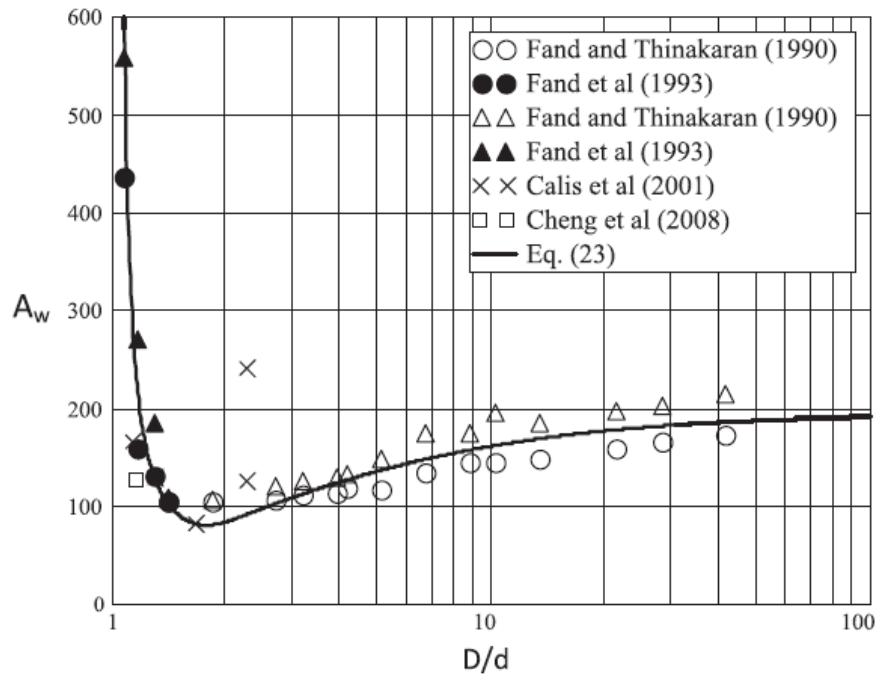


Fig. 4

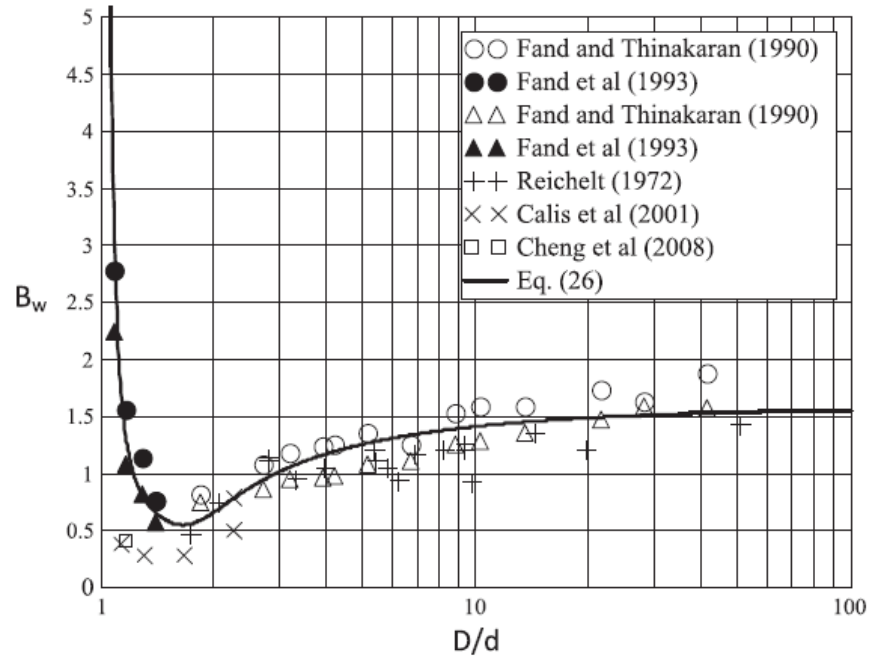


Fig. 5